

1969

# Pilot study on the fatigue of tension specimens (phases 1 and 2), October 1969

R. J. Smith

P. Marek

M. Perlman

A. W. Pense

Follow this and additional works at: <http://preserve.lehigh.edu/engr-civil-environmental-fritz-lab-reports>

## Recommended Citation

Smith, R. J.; Marek, P.; Perlman, M.; and Pense, A. W., "Pilot study on the fatigue of tension specimens (phases 1 and 2), October 1969" (1969). *Fritz Laboratory Reports*. Paper 402.

<http://preserve.lehigh.edu/engr-civil-environmental-fritz-lab-reports/402>

This Technical Report is brought to you for free and open access by the Civil and Environmental Engineering at Lehigh Preserve. It has been accepted for inclusion in Fritz Laboratory Reports by an authorized administrator of Lehigh Preserve. For more information, please contact [preserve@lehigh.edu](mailto:preserve@lehigh.edu).



Low Cycle Fatigue Behavior  
Of Joined Structures

# PILOT STUDY ON THE FATIGUE OF TENSION SPECIMENS (PHASES 1 AND 2)

FRITZ ENGINEERING  
LABORATORY LIBRARY

by  
R. J. Smith, P. Marek  
M. Perlman, A. W. Pense  
K. H. Frank, J. W. Fisher

Fritz Engineering Laboratory Report No. 358.3

UNIVERSITY OF PITTSBURGH  
INSTITUTE OF RESEARCH

LOW CYCLE FATIGUE BEHAVIOR OF JOINED STRUCTURES

PILOT STUDY ON THE FATIGUE  
OF TENSION SPECIMENS  
(PHASES 1 AND 2)

by

R. J. Smith, P. Marek

M. Perlman, A. W. Pense

K. H. Frank, J. W. Fisher

This work was conducted as part of a study of low-cycle fatigue, sponsored by the Office of Naval Research, Department of Defense, under Contract N 00014-68-A-514; NR 064-509. Reproduction in whole or part is permitted for any purpose of the United States Government.

Department of Civil Engineering

Department of Metallurgy and Materials Science

Fritz Engineering Laboratory  
Lehigh University  
Bethlehem, Pennsylvania

October, 1969

Fritz Engineering Laboratory Report No. 358.3

TABLE OF CONTENTS

	<u>Page</u>
ABSTRACT	i
1. INTRODUCTION	1
2. EXPERIMENTAL PROGRAM	3
2.1 Experimental Design	3
2.2 Test Specimens	3
2.3 Testing Machines	5
2.4 Testing Procedure	5
2.5 Metallographic Examination	7
3. TEST RESULTS	8
3.1 Fatigue Life and Plastic Strain Accumulation	8
3.2 Metallographic Results	9
4. DISCUSSION	10
4.1 Effect of Variables	10
4.2 Statistical Analysis	13
4.3 Metallurgical Studies	14
5. CONCLUSIONS	17
6. ACKNOWLEDGEMENTS	19
7. NOMENCLATURE	21
8. TABLES AND FIGURES	22
9. REFERENCES	49

ABSTRACT

This report presents a summary and evaluation of the results of a pilot study, which is part of a major research program designed to provide information on the behavior and design of joined structures subjected to low-cycle fatigue.

Seventy-one tension specimens were tested to obtain information on the significance of several design factors which may influence the fatigue life of A514 steel from about 10,000 up to 100,000 cycles. In addition, experience was gained concerning the method of testing and the instrumentation required for later tests.

The fracture surfaces were characterized and correlations of fatigue life with maximum stress and stress range were tested. When the maximum stress was below the proportional limit it was determined statistically that the stress range accounts for nearly all the variations in cycle life. In regions of high maximum applied stresses, the test data was not sufficient for statistical predictions concerning the effect of the applied stress parameters upon fatigue life.

Final fracture of the specimens was initiated by flat fatigue cracks and proceeded by non-homogeneous plastic flow across the specimen. At high loads and high stress

ranges, multiple crack initiation was observed and the flat fatigue crack was a smaller portion of the critical fracture surface.

For high maximum stresses where "plastic damage" occurs during fatigue, the study has indicated that measurements of plastic strain accumulation during testing will be necessary.

## 1. INTRODUCTION

This report presents the results of a pilot study, which is part of a major research program designed to provide information on the behavior and design of joined structures subjected to low-cycle fatigue. The material studied was ASTM A514 Grades B and J steel.

The tests of this pilot study were conducted in two phases. The first phase of the investigation<sup>(1)</sup> was supplemented by additional tests to allow a satisfactory evaluation of the results. This report presents a summary and evaluation of the results of both phases.

The purpose of this pilot study was to gain experience concerning methods of testing and application of instrumentation prior to undertaking future tests on plain and welded specimens. It was carried out to obtain initial information on the significance of several design factors which may influence the life of A514 steel under cyclic loading in the most significant region of the tension-tension stress range. The design factors of major interest in this study are the effects of maximum applied stress,  $S_{\max}$ , and applied stress range,  $S_r$ , and the suitability of the proposed specimen configuration.

A study of previous investigations has indicated

that most low-cycle fatigue tests are strain controlled. However, because of the available testing machine, the tests in this pilot study were performed at constant load amplitude.



## 2. EXPERIMENTAL PROGRAM

### 2.1 Experimental Design

An experiment design was undertaken to permit a rational evaluation of the influence of the controlled variables on the fatigue lives of tensile specimens. The tests were restricted to high maximum tensile stresses and stress ranges resulting in tension-tension testing. The objective of the experiment was to evaluate the significance and interaction of the controlled variables. Table 1 describes the experimental factorial in terms of the stress variables.  $S_{\max}$  is the maximum applied stress and  $S_r$  is the applied stress range. The magnitudes of  $S_{\max}$  and  $S_r$  were selected on the basis of previous studies<sup>(2)</sup> and corresponded to fatigue lives up to an estimated 100,000 cycles.

Replication of specimens within each test cell provides a measure of the error variation and increases the sensitivity of the factorial with respect to variations in fatigue data.

### 2.2 Test Specimens

The program consisted of testing 71 specimens of

A514 Grades J and B steel. The specimen material was oxygen-cut from the flanges of nine beams previously tested in high-cycle fatigue.<sup>(3)</sup> Most of the specimens were obtained from flange areas of low applied stress (shear spans) and low residual stress.<sup>(4)</sup> Figure 1 shows the beam loading and the portion of the flange from which the specimens were taken. Lateral surfaces of the specimens were left as-rolled and fillets for the reduced section were not smoothed after machining. The specimen configuration is shown in Fig. 2 and a summary of the specimen dimensions is listed in Table 2. The specimen notation was derived from the beam designation system previously used.<sup>(3)</sup> In Table 2,  $b$  is the width,  $t$  is the thickness, and  $A$  is the area of the specimen.

A summary of the previous high-cycle fatigue history of the nine beams is given in Table 3. In this table, the beam designation, the number of cycles of loading and the applied stress parameters  $S_{\max}$  and  $S_r$  are given. Since the tension specimens were cut from the shear span, it is estimated that the specimens were subjected to average stresses much smaller than the applied stress parameters of Table 3.

Table 4 summarizes the mechanical properties obtained from laboratory tension tests performed on four specimens cut from these beams. The specimen configuration for the

tension tests was that shown in Fig. 2. In Table 4,  $\sigma_p$  is the proportional limit,  $\sigma_{yd}$  is the dynamic yield stress using a strain rate of 0.025 in./min.<sup>(5)</sup>,  $\sigma_{ys}$  is the static yield stress,  $\sigma_u$  is the ultimate tensile stress and E is Young's Modulus. Figure 3 shows a stress-strain curve traced from the tension test using a two inch gage length on specimen PWC-142-5.

### 2.3 Testing Machines

The fatigue tests were conducted in 200 and 250 Kip Alternating Stress Machines. The machine applies the alternating load, by hydraulic means, to the specimen which is gripped with a set of cross-cut jaws.

The laboratory tension tests were performed in a 120 Kip Static Testing Machine.

### 2.4 Testing Procedure

The specimen was first placed in the machine grips. It was then loaded statically to the maximum stress to be used in the fatigue test to seat the grips. Where  $S_{min}$  was close to zero the grips were prestressed to prevent slippage. Thereafter the alternating load was applied to the specimen until the desired maximum applied stress and

range of applied stress were obtained. The frequency of the alternating load for each test was set at either 250, 350 or 500 cycles per minute depending on the expected fatigue life. The number of cycles were accumulatively recorded by a counter on the machine. Counting started only after the designated applied stress range was reached. This took between 400 to 1000 cycles to achieve and is not included in the data. Crack arrest marks on the fracture surfaces showed that the machine did not maintain the maximum load during rapid crack extension. The machine was therefore set to detect an approximately ten percent decrease in load to stop the machine. This was defined as failure. Counting continued for 400 to 600 cycles after the specimen failed as the machine coasted to a stop. These cycles were included in the data because they equal approximately the number of cycles needed for adjustment of the desired stress range at the beginning of the test.

The order of testing was randomized to prevent systematic errors and bias due to uncontrolled variables. All specimens were tested at room temperature.

An attempt was made to measure accumulation of plastic strains by attaching strain gages to a few specimens and using an oscilloscope for measurement and by linear measurement of distance between scribed lines on the specimen surface.

## 2.5 Metallographic Examination

The specimens after testing were examined for macroscopic appearance of the fracture surface. Sections were made through selected typical fracture surfaces and examined after standard metallographic preparation. The fatigue initiation region and the final fracture surface were characterized.

### 3. TEST RESULTS

#### 3.1 Fatigue Life and Plastic Strain Accumulation

Table 5 presents a summary of the test program during which additional tests were required. The specimens in which the maximum applied stress was 102 ksi resulted from keeping the applied stress range constant at 99 ksi while the minimum obtainable stress due to the necessary loading arrangement was 3 ksi.

The fatigue test data are presented in Table 6. The frequency of alternating load, the number of cycles to failure, and the approximate location of the fracture for each fatigue specimen are given. Figure 4 defines the approximate region of fracture.

Figure 5 is a log-log plot of the applied stress range versus the number of cycles to failure for the data of Table 6.

Table 7 summarizes plastic strain accumulation. In this table, the specimen number, the number of cycles and the accumulated strain are given. For specimen PWC-142-6 these data were obtained from strain gage measurements. These measurements were recorded until the strain gage became damaged. The gages on four other specimens failed after a few cycles, as the maximum stress caused strain beyond the range the gages could record. The final elongation for specimens

PWC-142-1 and PWC-142-3 were obtained by direct measurement between scribed lines on the specimen surface.

### 3.2 Metallographic Results

Macroscopic examination of the fracture surfaces of the test specimens is summarized in Table 8.

Selected fracture surfaces are shown macroscopically in Fig. 6. Planes for sectioning and polishing are indicated.

A section showing a change in the nature of the fatigue fracture surface is shown in Fig. 7. The fracture surface shows no delamination tendency at surface start (top of Fig. 7) with a gradual change to severe delaminations. Transition from flat fatigue fracture to a slant fracture mode is shown in Fig. 8.

Typical macroscopic features of the test samples are shown in Fig. 9. A polished section through one specimen to illustrate multiple fatigue crack initiations is shown in Fig. 10.

#### 4. DISCUSSION

##### 4.1 Effect of Variables

For some specimens in Table 6 the number of cycles to failure were either low or high as compared to other specimens of the same category. The low values may have resulted from the effects of either initial flaws such as inclusions, cracks from previous cyclic load history, scribed lines, or misalignment of the specimens in the machine grips.

Variations in fatigue life may have been influenced by the number of low-stress cycles and loading conditions while these specimens were tested previously as portions of the flanges of high-cycle fatigue beams. Two different types of A514 steel were tested. Therefore metallurgical effects might have influenced the test data.

Failure was definitely affected by the stress concentrations produced by the specimen configuration. Most failures occurred at the machined radius of the specimen.

A high fatigue life for a specimen within a cell may have resulted from load variations during testing. The machine load is difficult to keep adjusted and



tends to decrease by approximately three to five percent from the required maximum load. Consequently, the applied stress parameters may have been less than the recorded stresses. Since fatigue life is very sensitive to maximum stresses close to ultimate stress,<sup>(2)</sup> a slight decrease in the alternating load would result in a substantial increase in the specimen fatigue life.

As was expected from high-cycle fatigue behavior, the applied stress range had a substantial effect upon cycle life. An increase in stress range was accompanied by a decrease in the number of cycles to failure.

It is visually apparent from Fig. 5 that the log transformation of life and stress range may result in an approximate linear relationship between these two variables. It also indicated that the number of cycles to failure of specimens tested at maximum applied stresses of 80 and 90 ksi are approximately the same as specimens tested at 100 (or 102) ksi when the stress range was the same. Since these maximum stresses are below the proportional limit, the tests conducted were also constant strain tests. Hence, stress range apparently accounts for nearly all the variation in cycle life in this region.

When the maximum stress,  $S_{\max}$  was increased above the proportional limit (varies between 101.3 to 105.2 ksi) most of the test data tended to shift to lower lives than

for other levels of maximum stress. An examination of Fig. 5 shows that this observation is not applicable to all levels of stress range. At 62, 75 and 99 ksi levels of stress range, a few specimens at a maximum stress of 100 ksi had comparable lives. However, specimens which show this behavior may have reduced fatigue lives due to the previously mentioned factors influencing cycle life. The data suggest that at applied stress levels above the proportional limit the maximum applied stress may have some influence upon the expected number of cycles to failure. This behavior is contrary to the results of high-cycle low stress fatigue where the maximum applied stress has usually no effect upon the number of cycles to failure.<sup>(6)</sup>

Figure 11 summarizes the strain history data of Table 7 in the form of a log-log plot of the percent strain versus the number of cycles. Each solid circle represents a recorded data point. The measured plastic strain accumulation is represented by the heavy dashed lines joining the solid circles and the assumed behavior is shown by the light dashed lines. It is apparent from Fig. 11 that only a small amount of plastic strain occurred during most of the fatigue life. Substantial increases were observed only in the first few cycles of life and near failure.

Figure 12 is a graph of maximum applied stress,  $S_{\max}$ , non-dimensionalized as  $S_{\max}/\sigma_u$ , versus average number of

cycles to failure. Each solid circle or square represents an average value of the fatigue life for a cell of the total experiment. The assumed behavior as observed from a previous report,<sup>(2)</sup> is given by the dashed lines for each applied stress range. However, the scope of this pilot study as indicated in Fig. 13 was just a small part of the possible low-cycle fatigue range.

#### 4.2 Statistical Analysis

The test data was statistically analyzed using the methods of variance and regression analysis. The life of the specimens was transformed to the logarithm of their lives for the analysis.

An analysis of variance was performed on only two factorials contained within the total experiment as shown in Table 9. In Table 9, the levels of the two variables, stress range and maximum stress, and the fatigue lives of the specimens analyzed are given. Specimens in which failure occurred in the gripped portion of the specimen were not considered in the analysis.

The results of the analysis are given in Table 10. Stress range was significant at the five percent level of significance in both factorials. The effect of maximum stress was statistically insignificant in both factorials investigated.

The interaction of maximum stress and stress range was significant in Factorial I. The interaction of the two independent variables was also evident in Factorial II.

The results of a regression analysis are given in Table 11. All specimens were included in the analysis. The various models fitted to the test data including stress range are seen to give the best fit. The sum of squares reduced by maximum stress was insignificant for all models which included stress range and maximum stress as variables.

Figure 14 summarizes the results of the regression analysis in the form of a graph of  $S_{\max}/\sigma_u$  versus number of cycles to failure. The data points represent an average value of the fatigue life for a cell and the dashed lines represent the predicted behavior of the fitted models. These models apply only to the area investigated by the statistical analysis as indicated in Fig. 14. Thus this test data is not sufficient for statistical conclusions concerning fatigue tests conducted in regions where accumulation of plastic strains occur during fatigue.

#### 4.3 Metallurgical Studies

All fracture surfaces show a dual character. They have a flat fracture area indicative of fatigue cracks of quarter circle (at edges) or semi-circular (at lateral

surfaces) shape. They are normal to the specimen surfaces. When these cracks reach a given size, by joining or growth, failure proceeds during very few cycles relative to the specimen life, accompanied by non-homogeneous plastic flow in the remaining section. Arrest marks are often observed in this latter stage of fracture as a result of the cyclic loading of the testing machine which stops the growing fracture during its unloading cycle (see Fig. 6).

The area occupied by the flat fatigue portion of the fracture decreased as both stress range and maximum load increased. Table 8 is a summary of the macroscopic appearance of the fracture surfaces.

Multiple flat fatigue crack initiations were observed at each of the maximum stresses or stress ranges. There were more of them evident, however, at higher maximum stresses and stress ranges.

The portion of the fracture surface outside the flat fatigue section is generally normal to the surfaces with a fibrous center and arrest marks along the edges when the stress range is 52 or 62 ksi. At higher maximum stresses or stress ranges the nonflat fracture region is inclined (slanted) to the lateral surfaces of the specimen. This slant surface is slightly fibrous in the center and can show arrest marks at the edges.

Sections polished through the flat fatigue and secondary fracture surfaces revealed similar features in the same characteristic region as illustrated in Figs. 7, 8 and 10. The size of flat fatigue initiation areas changes with maximum stress and stress range as mentioned above. The polished sections in Fig. 7 show that the initial flat fatigue crack showed no tendency to delaminate along rolled-out inclusions. At greater crack depths normal to the specimen surface, delamination becomes pronounced. When the secondary (slant) fracture region is reached there is no significant delamination as illustrated in Fig. 8.

Flat fatigue cracks either started singly or multiply at corners or along the surface of the specimen. Figures 9a and 9b show multiple flat fatigue cracks which joined through a delamination step or through slant fracture. Figure 9c shows edge fatigue cracks which were opened by the non-homogeneous plastic flow preceding final failure. Most fractures started at the end of the machined fillet at the reduced test section. An edge crack at a fillet which did not become part of the critical fracture path is shown in Fig. 9d. Cracks present on planes other than the main fracture surface are revealed in the polished section as shown in Fig. 10. Two of these cracks are shown after etching in Figs. 10a and 10b. These cracks are normal to the plate surface and run across rolled-out inclusions without delaminating along them.

## 5. CONCLUSIONS

This report presents the results of two phases of a pilot study, which is part of a major research program designed to provide information on the behavior and design of welded structures under low-cycle fatigue.

The purpose of this pilot study was to obtain initial information on the significance of several design factors which may influence the life of A514 steel under cyclic loading in the tension-tension stress range. In addition, experience was gained concerning methods of testing and application of instrumentation required for future tests. The following conclusions were reached:

1. This study has indicated that stress range,  $S_r$ , accounts for nearly all the variation in cycle life when  $S_{max}$  is below the proportional limit.
2. The transformation of the logarithm of the cycle life with the logarithm of the stress range results in an approximate linear relationship between these two variables when the maximum applied stress is below the proportional limit.
3. The plastic strain accumulation or "plastic damage"

tends to decrease the fatigue life when  $S_{\max}$  exceeds the proportional limit.

4. The statistical methods of variance and regression analysis of the test data substantiated the importance of  $S_r$  on predicted high-cycle low stress fatigue behavior. There were not enough data for a statistical evaluation of the influence of high maximum stresses (plastic strains) on low-cycle fatigue.
5. Fracture was initiated by a flat fatigue crack followed by non-homogeneous plastic flow and fracture across the remainder of the specimen.
6. Higher maximum loads and stress range causes the flat fatigue crack section to be a smaller portion of the critical fracture surface.
7. Multiple flat fatigue crack initiation is encouraged by higher maximum loads and higher stress ranges.
8. Flat fatigue cracks show no tendency to delaminate near the surface and gradually increase their delamination tendency as they grow through the plate thickness.



## 6. ACKNOWLEDGEMENTS

The investigation is part of a major research program on low-cycle fatigue, and was conducted at Fritz Engineering Laboratory, Lehigh University, Bethlehem, Pennsylvania. One phase of the fatigue testing was carried out by Standard Pressed Steel Company Laboratories, Jenkintown, Pennsylvania. The Office of Naval Research, Department of Defense, sponsored the research under Contract N 00014-68-A-514; NR 064-509. The program manager for the overall research project is Lambert Tall.

The guidance of, and the suggestions from, the members of the special Advisory Committee on Low-Cycle Fatigue is gratefully acknowledged. The authors wish to thank Lambert Tall and Ben T. Yen for their helpful comments during the investigation and the preparation of the report and Salvador Lozano for his help during the testing program.

Sincere thanks are due to Joanne Mies who typed the report, to Jack M. Gera who prepared the drawings, and to Kenneth Harpel, Laboratory Superintendent, and his staff, for their assistance during testing.

Lynn S. Beedle is Director of Fritz Engineering Laboratory, and Joseph F. Libsch is Vice-President for Research, Lehigh University.

7. NOMENCLATURE

A	Area of specimen
b	Width of specimen
DOF	Degrees of freedom
E	Young's Modulus (ksi)
$F_{CALC}$	Stress Ratio Calculated (see Ref. 7)
$F_{TAB}$	Stress Ratio Tabulated (see Ref. 7)
N	Number of cycles to failure
$S_{max}$	Maximum applied stress (ksi)
$S_{min}$	Minimum applied stress (ksi)
$S_r$	Applied stress range (ksi)
t	Thickness of specimen
$\sigma_p$	Proportional limit (ksi)
$\sigma_u$	Ultimate stress (ksi)
$\sigma_{yd}$	Dymanic yield stress using a strain rate of 0.025 in./min.
$\sigma_{ys}$	Static yield stress (ksi)

8. TABLES AND FIGURES

TABLE 1 EXPERIMENTAL FACTORIAL

$S_{\text{max}} \backslash S_{\text{r}}$	80	90	100	106	109	112	115
52						3	
62		3	3*			3	
75	3	3	3	3	3	3	3
87		3	3	3	3	3	3
99			3			3	
109						3	
112							3

\*Number of specimens in cell

TABLE 2 SECTION DIMENSIONS\*

Specimen Number	b (in)	t (in)	A (in <sup>2</sup> )
311- 1	2.008	0.380	0.763
311- 2	2.009	0.380	0.763
311- 3	2.010	0.380	0.764
311- 4	2.009	0.380	0.763
311- 5	2.010	0.379	0.762
311- 6	2.010	0.380	0.764
311- 7	2.010	0.379	0.762
311- 8	2.010	0.380	0.764
311- 9	2.011	0.380	0.764
311-10	2.008	0.380	0.763
311-11	2.007	0.380	0.763
311-12	2.009	0.380	0.763
311-13	2.010	0.379	0.762
311-14	2.010	0.380	0.764
311-15	2.009	0.380	0.763
311-16	2.008	0.380	0.763
311-17	2.008	0.380	0.763
311-18	2.009	0.380	0.763
152- 1	2.004	0.392	0.786
152- 2	2.007	0.395	0.793
152- 3	2.006	0.394	0.790
152- 4	2.006	0.391	0.784
152- 5	2.005	0.392	0.786
152- 6	2.006	0.390	0.782
152- 7	2.005	0.394	0.790
152- 8	2.005	0.393	0.788
152- 9	2.005	0.394	0.790
152-10	2.005	0.394	0.790
142- 1	1.997	0.383	0.764
142- 2	1.999	0.385	0.770
142- 3	1.996	0.384	0.766
142- 4	1.998	0.383	0.765
142- 5	1.997	0.382	0.762
142- 6	1.998	0.382	0.763
142- 7	2.001	0.382	0.764
142- 8	2.001	0.384	0.768

\*See Figure 2

TABLE 2 CONTINUED

Specimen Number	b (in)	t (in)	A (in <sup>2</sup> )
312-1	1.997	0.390	0.778
312-2	1.996	0.391	0.780
312-3	2.004	0.391	0.783
312-4	2.004	0.390	0.782
141-1	1.996	0.420	0.838
141-2	1.995	0.391	0.780
141-3	1.996	0.400	0.798
141-4	1.996	0.392	0.782
141-5	1.996	0.389	0.776
141-6	2.002	0.390	0.781
141-7	1.996	0.397	0.792
141-8	1.996	0.422	0.842
242-1	2.001	0.385	0.770
242-2	2.004	0.388	0.778
242-3	2.004	0.389	0.780
242-4	1.997	0.389	0.776
242-5	2.003	0.388	0.778
242-6	2.004	0.388	0.778
242-7	2.006	0.387	0.776
242-8	1.997	0.389	0.776
131-1	1.997	0.391	0.780
131-2	1.997	0.395	0.788
131-3	1.997	0.395	0.788
131-4	1.997	0.396	0.789
341-1	1.996	0.381	0.760
341-2	1.996	0.382	0.762
341-3	2.001	0.382	0.764
341-4	2.000	0.382	0.764
341-5	1.997	0.382	0.762
341-6	1.996	0.382	0.762
341-7	1.999	0.384	0.768
341-8	1.997	0.383	0.764
321-1	1.996	0.382	0.762
321-2	1.995	0.379	0.756
321-3	2.006	0.382	0.766
321-4	2.004	0.380	0.762
321-5	1.996	0.380	0.758
321-6	2.002	0.379	0.758
321-7	2.002	0.379	0.758
321-8	1.996	0.381	0.760

TABLE 3 HIGH-CYCLE FATIGUE HISTORY

Beam Designation*	Number of Cycles of Loading ( $\times 10^3$ )	$S_{\max}$ (ksi)	$S_r$ (ksi)
CRC 141 (B)	341	14	20
CRC 131 (B)	515	10	16
PWC 311 (J)	2370	32	18
PWC 152 (J)	400	32	42
PWC 341 (J)	319	50	36
PWC 321 (J)	1318	38	24
PWC 142 (J)	561	26	36
CWC 312 (J)	2916	18	8
CWC 242 (J)	339	22	20

\*J or B indicate type of A514 steel

TABLE 4 MECHANICAL PROPERTIES

Specimen Number	$\sigma_p$ (ksi)	$\sigma_{yd}$ (ksi)	$\sigma_{ys}$ (ksi)	$\sigma_u$ (ksi)	E (ksi)
PWC-152-10	101.3	113.9		119.1	27900
PWC-311- 9	104.8	114.8		119.2	28400
PWC-142- 5	105.0	115.3	113.2	123.5	28100
CRC-141-2	105.2	119.6	117.1	125.9	27500



TABLE 5 COMPLETED TESTS

$S_{\max}$ / $S_r$	80	90	100 (102)	106	109	112	115
42						1	
52						5	
62		3	3			4	
75	3	3	3	4	3	3	3
87		3	3	3	4	3	3
99			(3)			3	
109						4	
112							4

TABLE 6 SUMMARY OF DATA

Specimen Number	S <sub>max</sub> (ksi)	S <sub>r</sub> (ksi)	Frequency of Alternating Load (cycles/min.)	Number of Cycles to Failure (x10 <sup>3</sup> )	Location of Fracture*
312- 1	80	75	350	111.0	End
242- 5	80	75	350	130.0	End
341- 7	80	75	350	104.3	Center
341- 2	90	62	350	252.6	End
321- 1	90	62	350	291.0	End
321- 4	90	62	350	135.2	In Grips
141- 4	90	75	350	97.3	End
141- 8	90	75	350	89.0	End
341- 4	90	75	350	118.4	End
311-12	90	87	250	77.5	End
311- 5	90	87	250	63.1	End
311- 4	90	87	250	63.7	End
341- 3	100	62	350	189.2	End
321- 5	100	62	350	126.2	End
312- 2	100	62	350	194.7	End
152- 7	100	75	250	139.5	End
152- 5	100	75	250	135.3	End
152- 2	100	75	250	75.2	End
152- 9	100	87	250	76.3	End
152- 4	100	87	250	84.8	Center
152- 1	100	87	250	62.0	Center
152- 8	102	99	250	56.9	End
152- 6	102	99	250	35.9	End
152- 3	102	99	250	23.9	End
321- 8	106	75	350	74.0	End
142- 8	106	75	350	84.0	End
142- 3	106	75	350	81.2	End
321- 3	106	75	350	74.5	In Grips
341- 6	106	87	350	60.4	End
142- 6	106	87	350	62.0	End
321- 2	106	87	350	64.5	In Grips
141- 3	109	75	350	106.3	End
242- 4	109	75	350	60.0	End
242- 8	109	75	350	85.3	End
141- 6	109	87	350	45.6	End
242- 1	109	87	350	60.0	End
131- 2	109	87	350	38.6	End
142- 2	109	87	350	74.2	End
311-11	112	42	500	732.8	End
311- 7	112	52	500	271.0	End

TABLE 6 SUMMARY OF DATA CONTINUED

Specimen Number	S <sub>max</sub> (ksi)	S <sub>r</sub> (ksi)	Frequency of Alternating Load (cycles/min.)	Number of Cycles to Failure (x10 <sup>3</sup> )	Location of Fracture*
311- 3	112	52	500	116.3	Center
341- 8	112	52	350	191.9	End
321- 7	112	52	350	221.6	End
142- 7	112	52	350	262.2	End
311- 6	112	62	250	127.2	End
141- 5	112	62	350	123.1	End
341- 5	112	62	350	130.5	End
321- 6	112	62	350	128.2	End
311- 2	112	75	250	94.6	Center
311-15	112	75	250	92.1	End
311-10	112	75	250	71.1	End
311-17	112	87	250	49.7	End
311-18	112	87	250	48.2	End
311-13	112	87	250	47.8	End
311- 1	112	99	250	31.8	End
311-16	112	99	250	39.0	End
311-14	112	99	250	43.8	End
311- 8	112	109	250	22.4	End
141- 1	112	109	350	22.5	End
242- 7	112	109	350	22.9	End
131- 1	112	109	350	20.0	End
141- 7	115	75	350	105.5	End
242- 3	115	75	350	81.2	End
341- 1	115	75	350	66.0	End
312- 3	115	87	350	38.1	Center
242- 2	115	87	350	39.0	End
131- 4	115	87	350	39.0	End
312- 4	115	112	350	10.0	Center
242- 6	115	112	350	11.6	End
131- 3	115	112	350	18.4	End
142- 1	115	112	350	19.6	Center

\*See Figure 4

TABLE 7 PLASTIC STRAIN ACCUMULATION

Specimen Number	Number of Cycles ( $\times 10^3$ )	Accumulated Strain (%)
142-6	3.5	.426
	8.3	.428
	10.8	.430
	13.6	.434
	16.4	.440
	20.4	.450
	23.8	.462
	27.6	.478
	29.8	.496
	30.5	.512
	31.3	.716
	35.0	.770
	62.0 (Failure)	Not Recorded
142-1	19.6 (Failure)	7.96
142-3	81.2 (Failure)	5.69

TABLE 8 FRACTURE APPEARANCE OF FATIGUE SPECIMENS\*

$S_r$ \ $S_{max}$	80	90	100	106	109	112	115
52						Multiple initiations. Normal fracture surface.	
62		Single corner initiation. Normal fracture surface.	Single corner initiation. Normal to slant fracture surface.			Multiple initiations. Normal fracture surface.	
75	Multiple initiations. Slant fracture surface.	Single corner initiation. Normal to slant fracture surface.	Multiple initiations. Slant fracture surface.	Single corner initiation. Normal fracture surface.	Multiple initiations. Slant fracture surface.	Multiple initiations. Normal or slant fracture surface.	Multiple initiations. Slant fracture surface.
87		Multiple initiations. Slant fracture surface.	Multiple initiations. Slant fracture surface.	Multiple initiations. Normal to slant fracture surface.	Multiple initiations. Slant fracture surface.	Multiple initiations. Normal or slant fracture surface.	Multiple initiations. Slant fracture surface.
99			Single corner initiation. Slant fracture surface.			Multiple initiations. Slant fracture surface.	
109						Single corner initiation. Slant fracture surface.	
112							Multiple initiations. Slant fracture surface.

\*Normal and slant refer to the orientation of the fracture surface to the original specimen surfaces.

TABLE 9 FACTORIALS FOR VARIANCE

FACTORIAL I

$S_r \backslash S_{max}$	90		100	
	Specimen	N	Specimen	N
87	311-12	77.5	152-9	76.3
	311-5	63.1	152-4	84.8
	311-4	63.7	152-1	62.0
75	141-4	97.3	152-7	139.5
	141-8	89.0	152-5	135.3
	341-4	118.4	152-2	75.2
62	341-2	252.6	341-3	189.2
	321-1	291.0	321-5	126.2
		271.8*	312-2	194.7

FACTORIAL II

$S_r \backslash S_{max}$	106		109		112		115	
	Specimen	N	Specimen	N	Specimen	N	Specimen	N
87	341-6	60.4	141-6	45.6	311-17	49.7	312-3	38.1
	142-6	62.0	242-1	60.0	311-18	48.2	242-2	39.0
		61.2**	131-2	38.6	311-13	47.8	131-4	39.0
75	321-8	74.0	141-3	106.3	311- 2	94.6	141-7	105.5
	142-8	84.0	242-4	60.0	311-15	92.1	242-3	81.2
	142-3	81.2	242-8	85.3	311-10	71.1	341-1	66.0

\* Average of 341-2 and 321-1

\*\* Average of 341-6 and 142-6

TABLE 10 ANALYSIS OF VARIANCE

FACTORIAL I

Source of Variation	Sum of Squares	DOF	Mean Squares	F <sub>CALC.</sub>	F <sub>TAB.</sub> *
S <sub>r</sub>	0.7021	2	0.3511	45.53	3.89**
S <sub>max</sub>	0.0081	1	0.0081	1.05	4.75
Interaction	0.0641	2	0.0320	4.15	3.89**
Residual	0.0925	12	0.0077		
Total	0.8668	17	0.0510		

FACTORIAL II

Source of Variation	Sum of Squares	DOF	Mean Squares	F <sub>CALC.</sub>	F <sub>TAB.</sub> *
S <sub>r</sub>	0.3170	1	0.3170	61.83	4.49**
S <sub>max</sub>	0.0279	3	0.0093	1.81	3.24
Interaction	0.0382	3	0.0127	2.48	3.24
Residual	0.0820	16	0.0051		
Total	0.4651	23	0.202		

\* 5% Level of Significance

\*\* Significant Effect

TABLE 11 REGRESSION ANALYSIS

FITTED MODELS

$$(A) \text{ LOG } N = B_1 + B_2 S_r + B_3 S_{\text{max}}$$

$$(B) \text{ LOG } N = B_1 + B_2 S_r$$

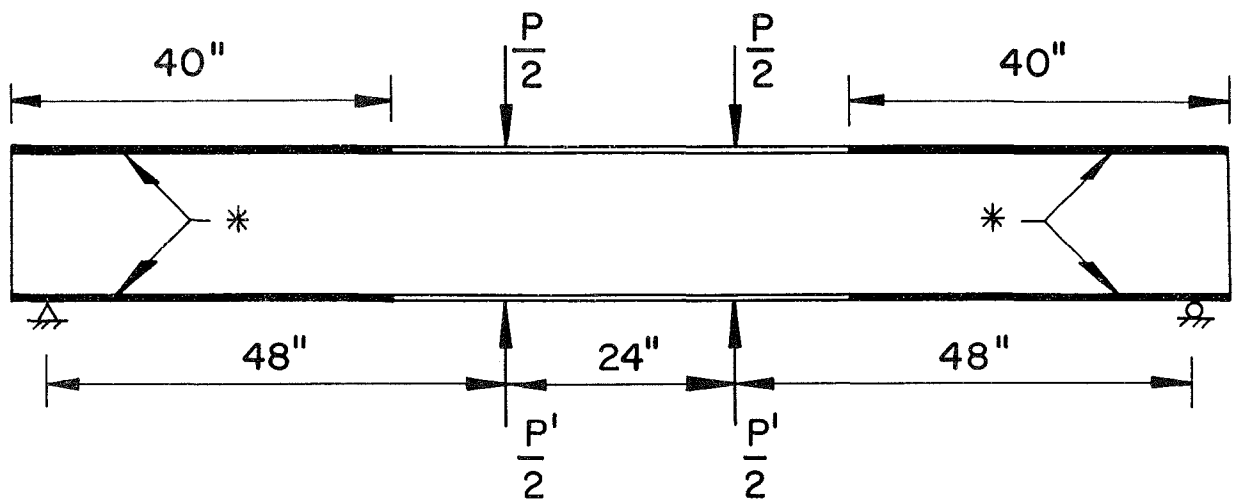
$$(C) \text{ LOG } N = B_1 + B_2 \text{LOG } S_r + B_3 \text{LOG } S_{\text{max}}$$

$$(D) \text{ LOG } N = B_1 + B_2 \text{LOG } S_r$$

REGRESSION RESULTS

Model	$B_1$	$B_2$	$B_3$	Correlation Coefficient	Standard Error of Estimate
A	3.97796	-0.01833	-0.00609	0.94890	0.10908
B	3.38659	-0.01896		0.93393	0.12265
C	11.5178	-3.23808	-1.74063	0.94806	0.10994
D	8.18835	-3.33762		0.92410	0.13113





\* Portion of beam flange from which specimens were obtained.

Fig. 1 Beam Loading and Specimen Location

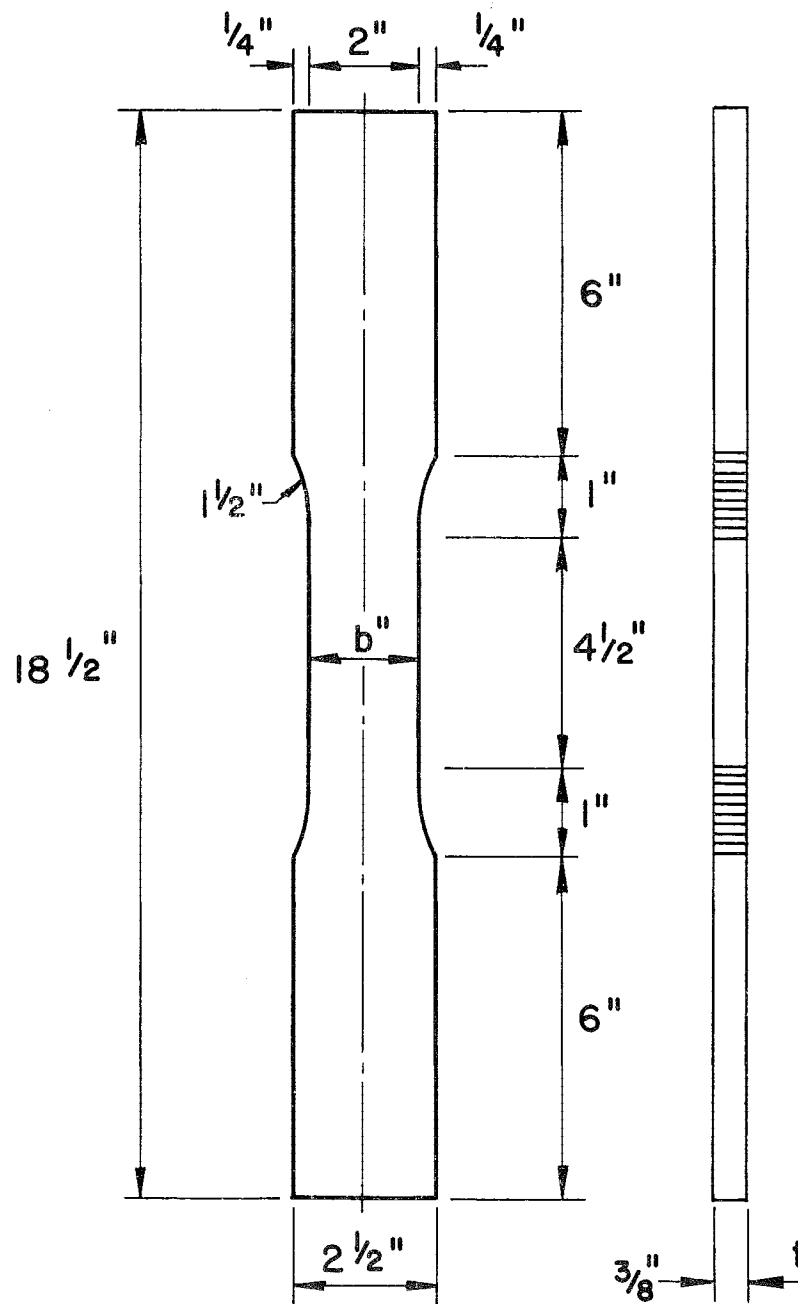


Fig. 2 The Shape of the Specimen

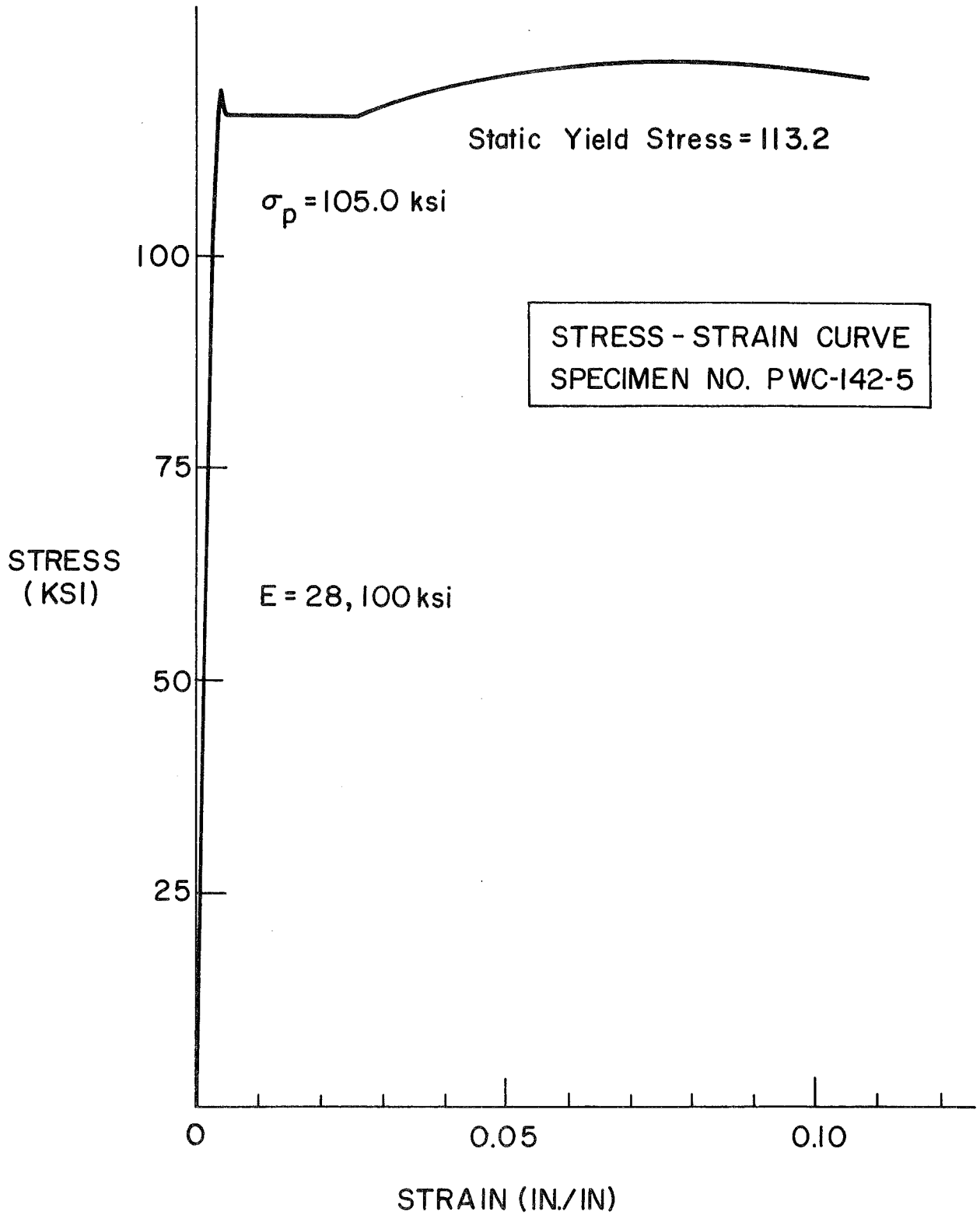


Fig. 3 The Stress-Strain Curve

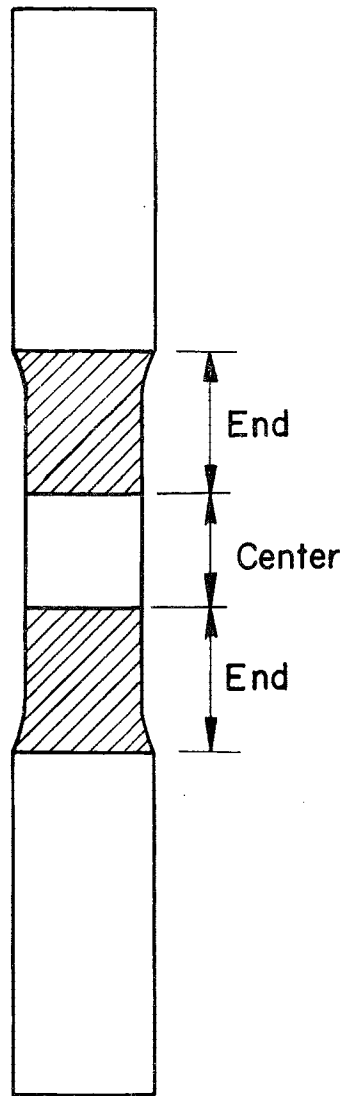


Fig. 4 Region of Fracture

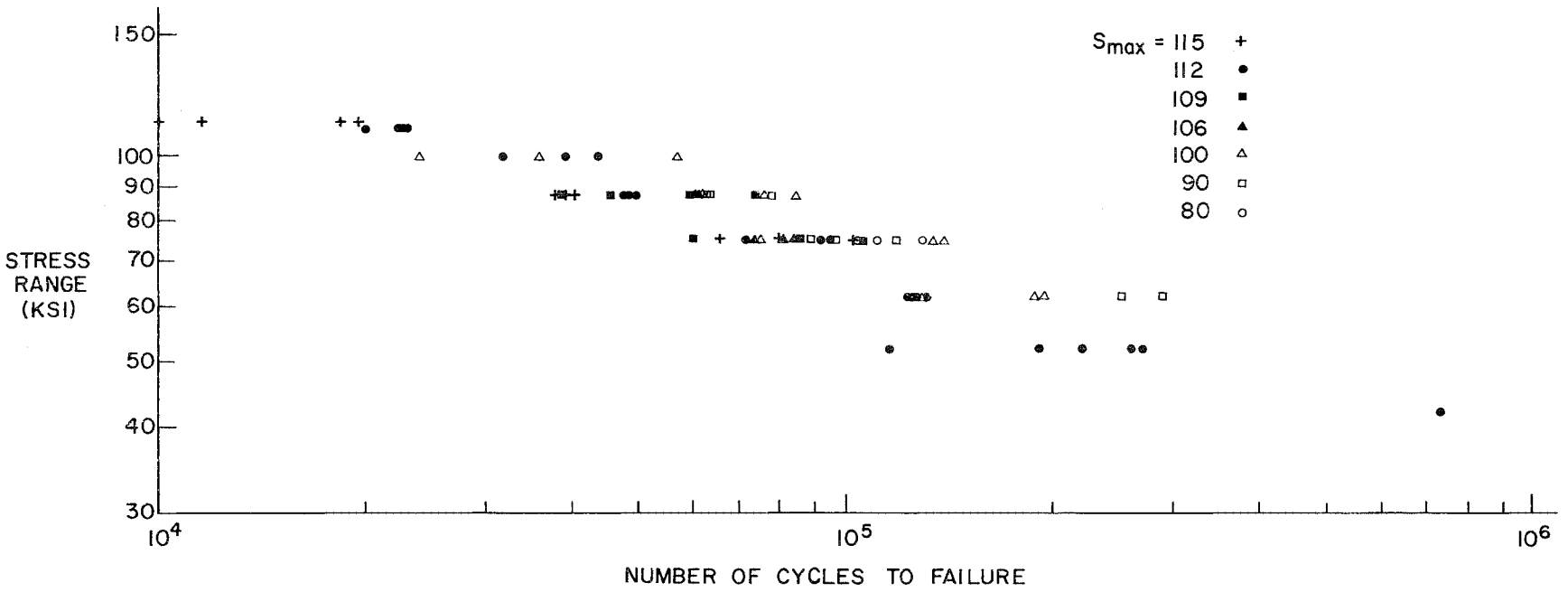
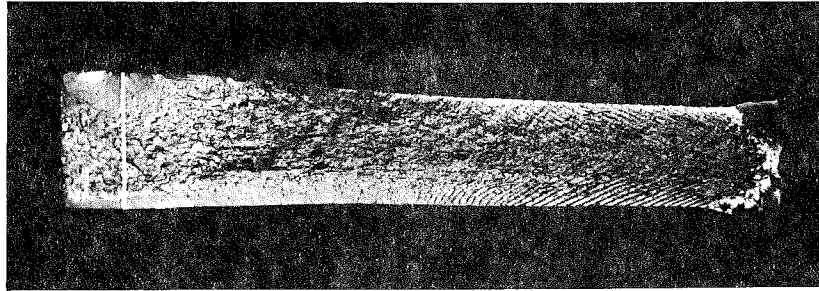
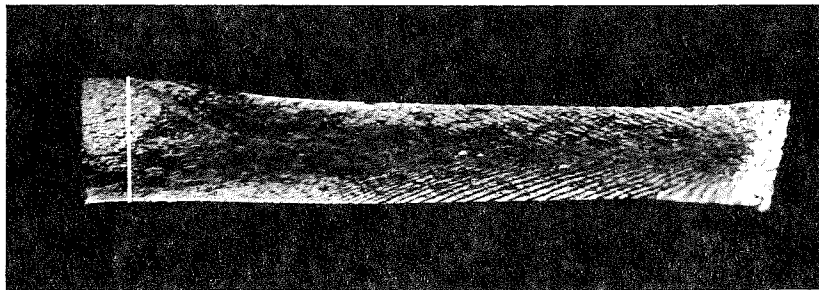


Fig. 5 Stress Range Versus Number of Cycles

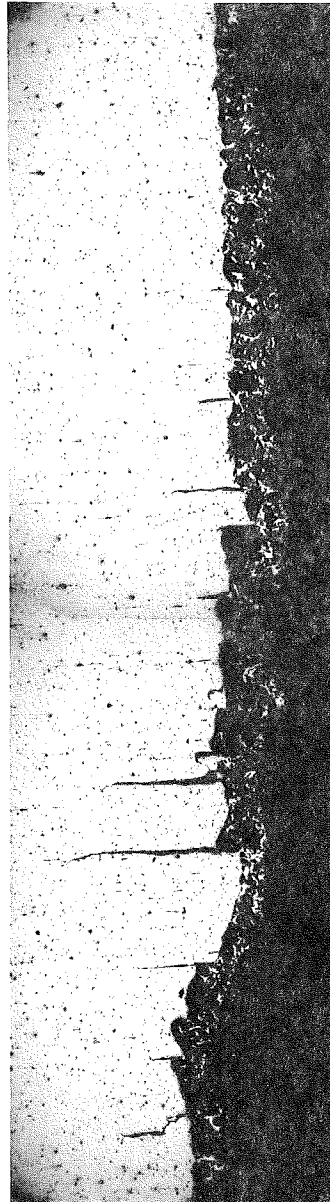


321-1



311-6

Fig. 6 Fracture Surfaces and Planes of Sectioning and Polishing



321-1

45x (Unetched)

Rolling Direction



Loading Direction

Fig. 7 Fatigue Crack Section

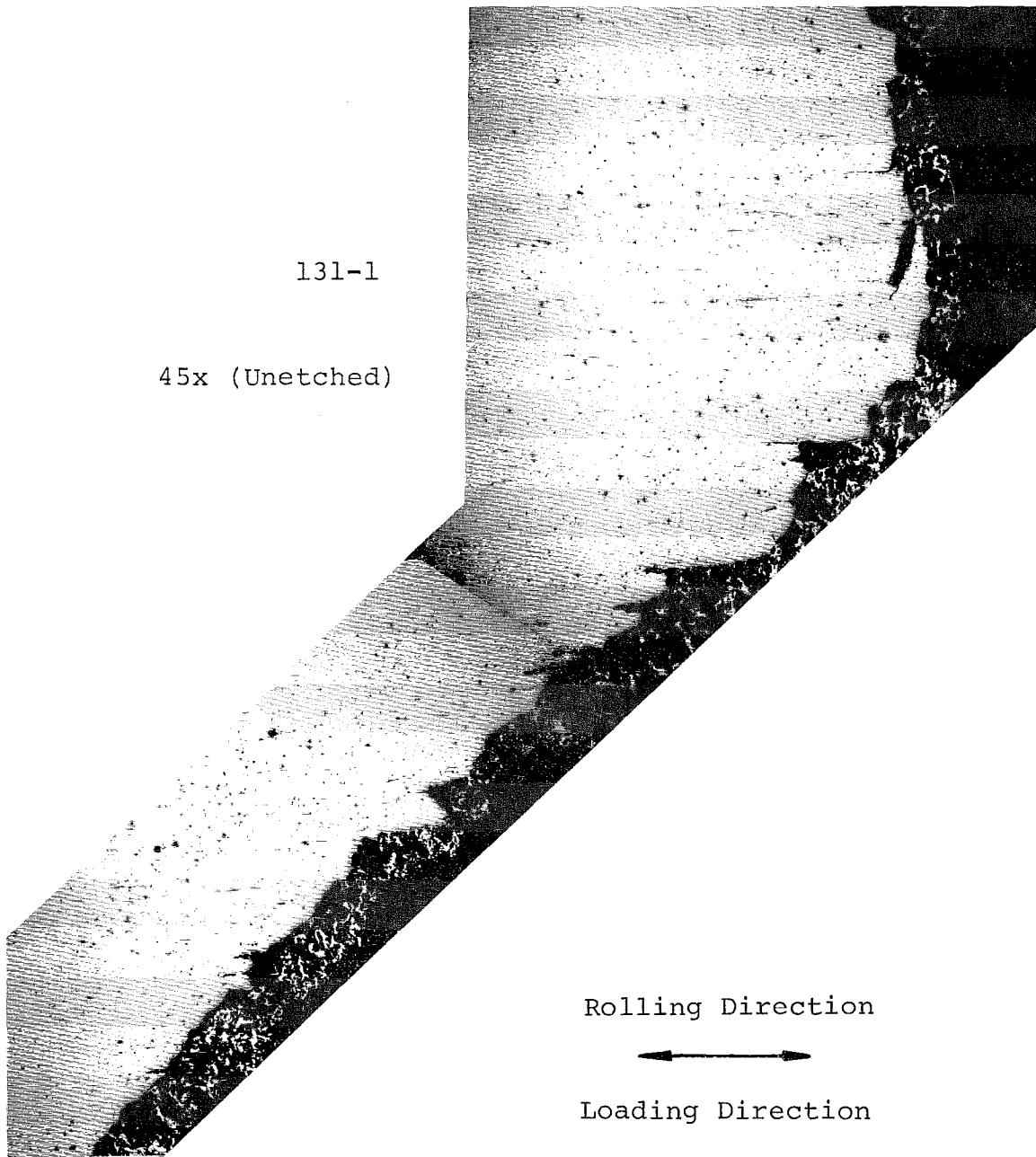


Fig. 8 Flat to Slant Fracture Section

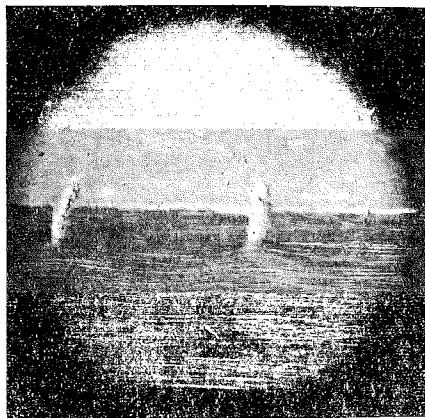




a Multiple Initiations



b Multiple Initiations

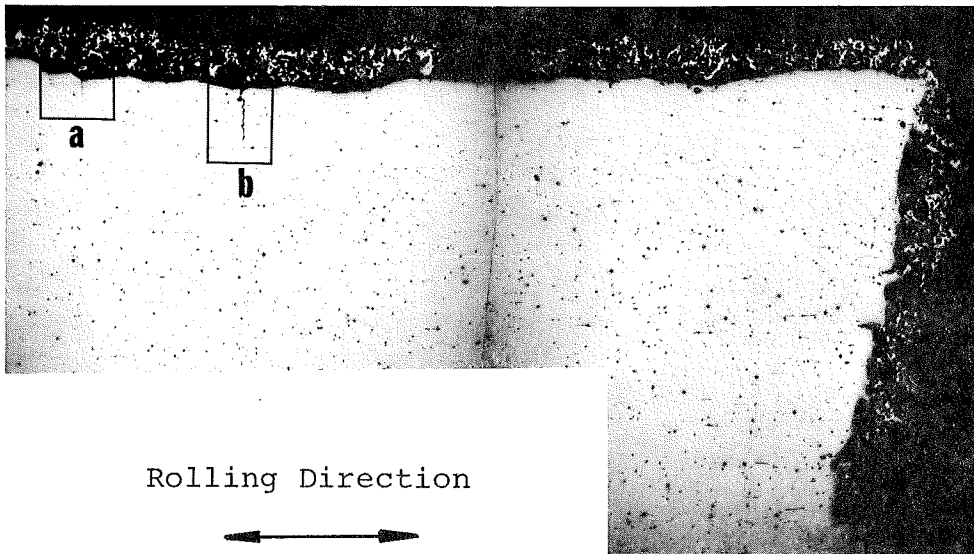


c Opening of Edge Cracks



d Cracks at Fillet

Fig. 9 Macroscopic Features



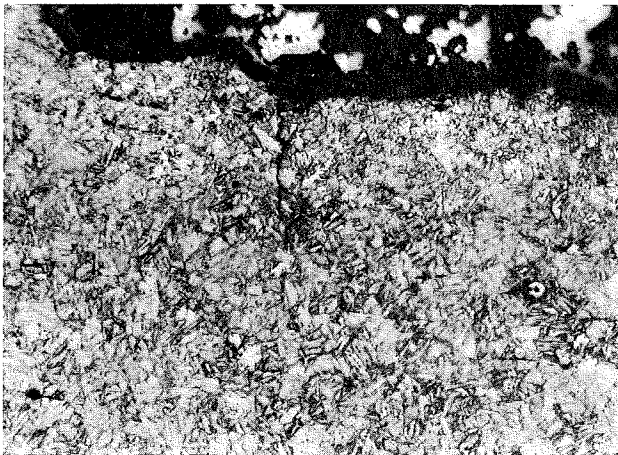
Rolling Direction



Loading Direction

131-1

45x



a 250x (Nital Etch)



b 250x (Nital Etch)

Fig. 10 Multiple Fatigue Crack Initiations

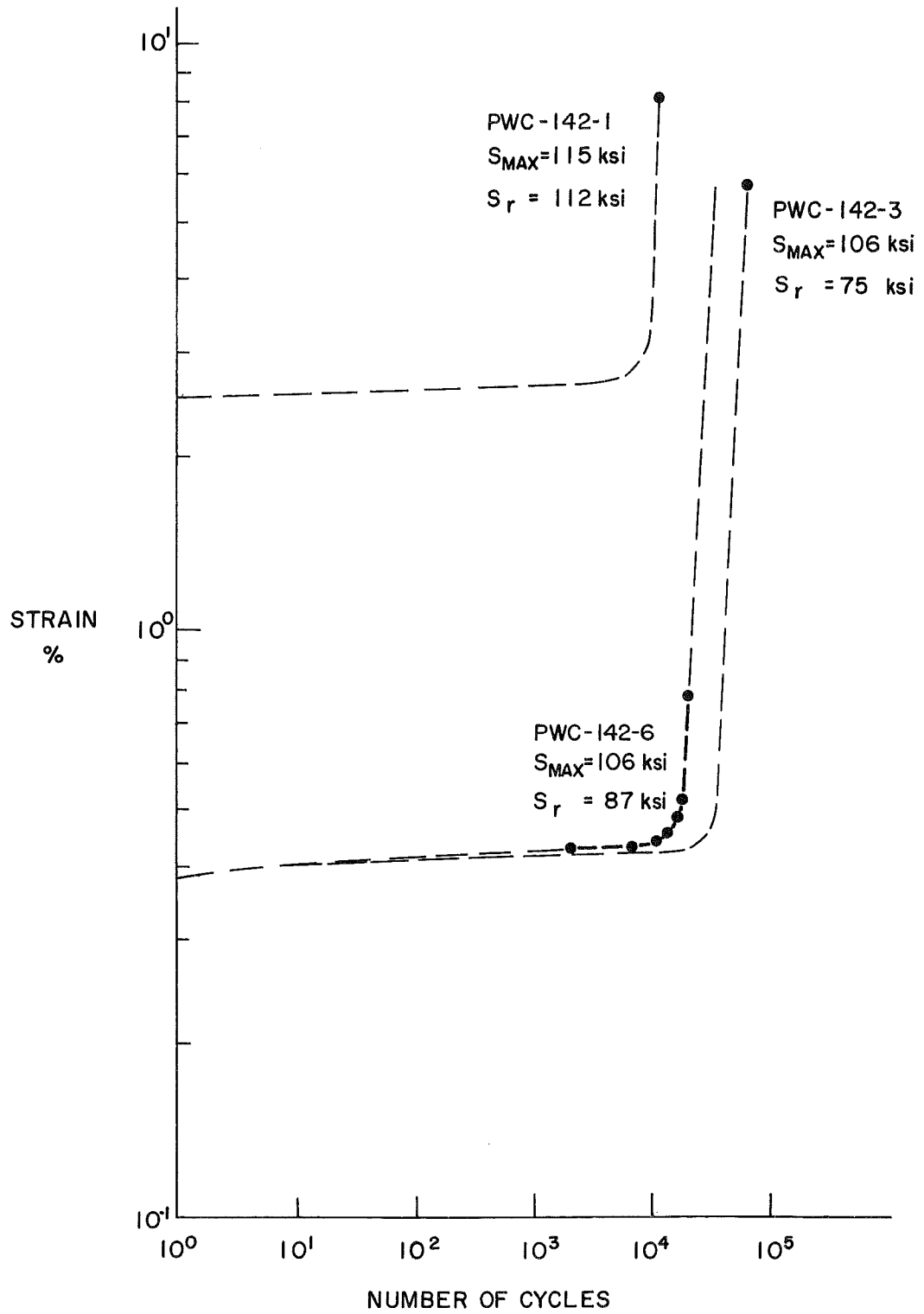


Fig. 11 Percent Strain Versus Number of Cycles

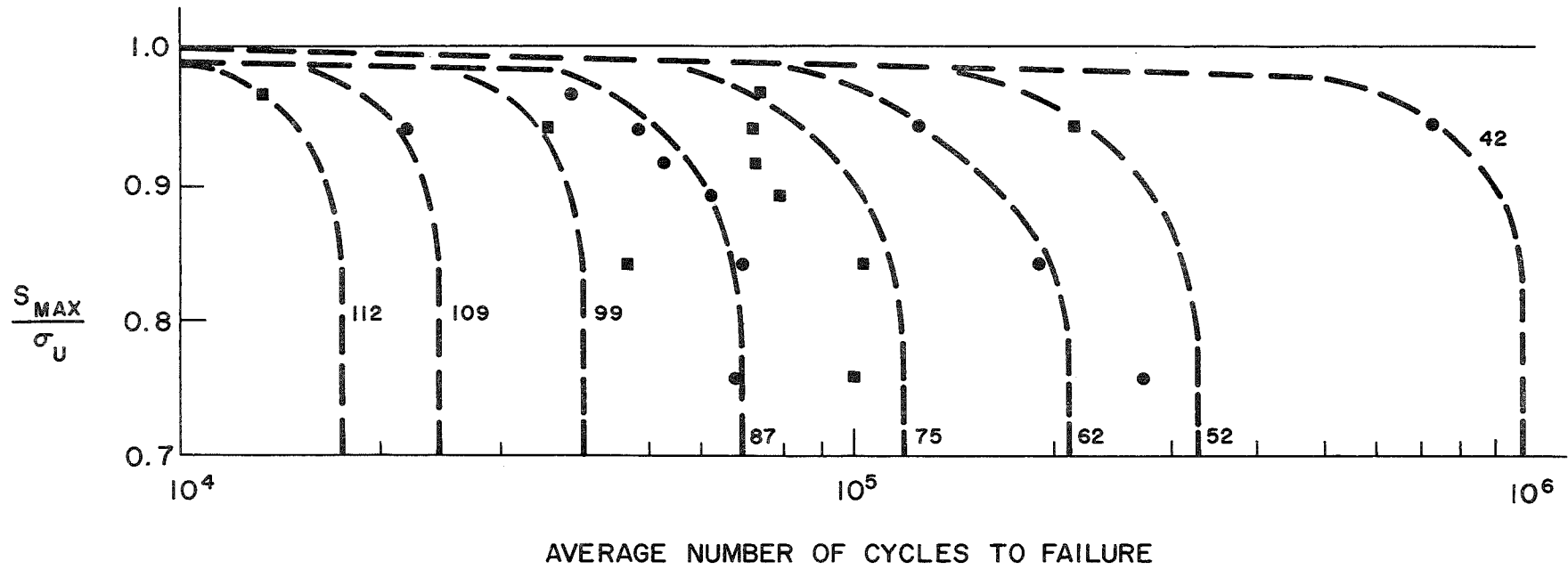


Fig. 12 Maximum Stress Ratio Versus Average Number of Cycles - Assumed Behavior

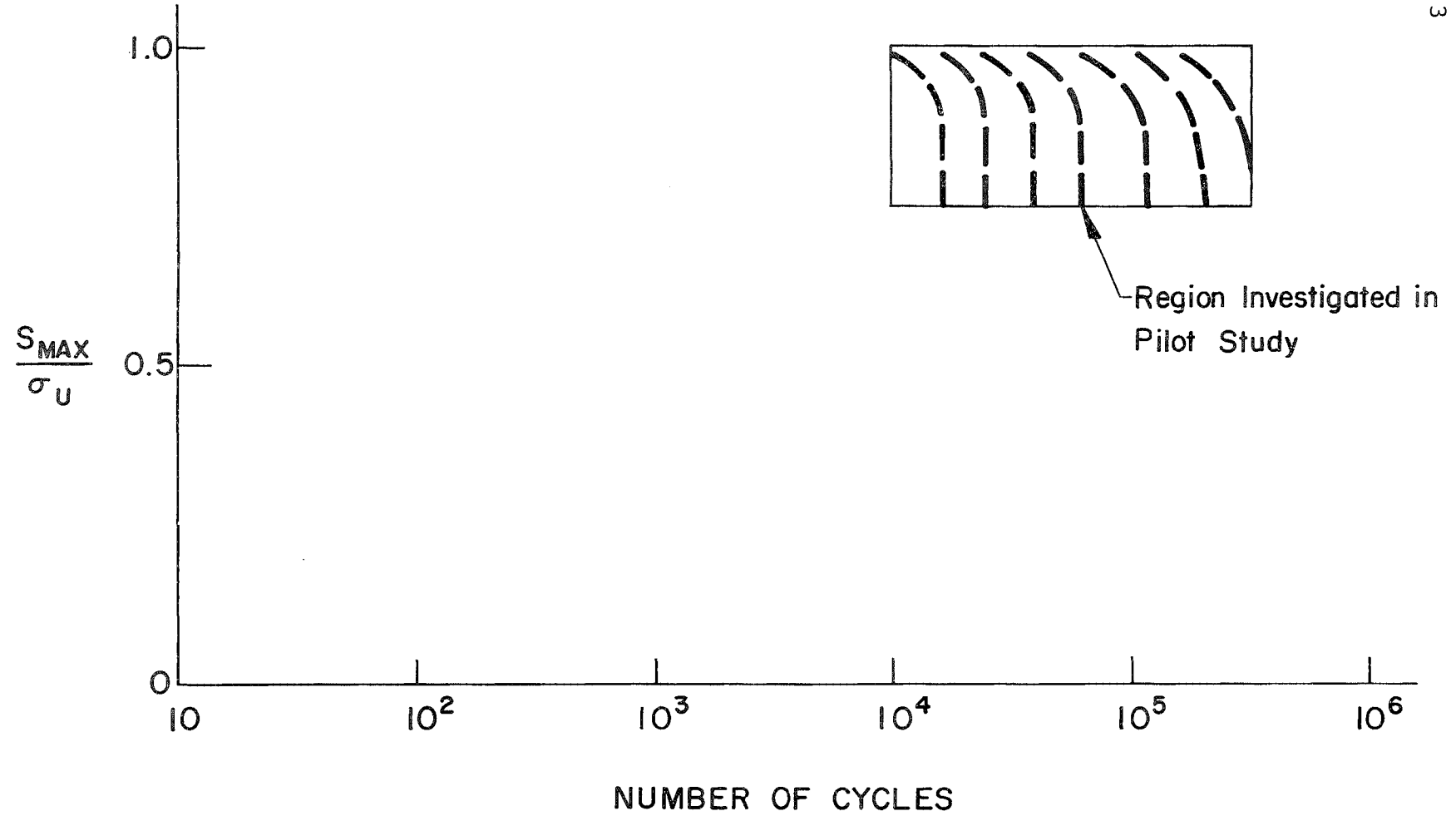


Fig. 13 Region Investigated in Pilot Study

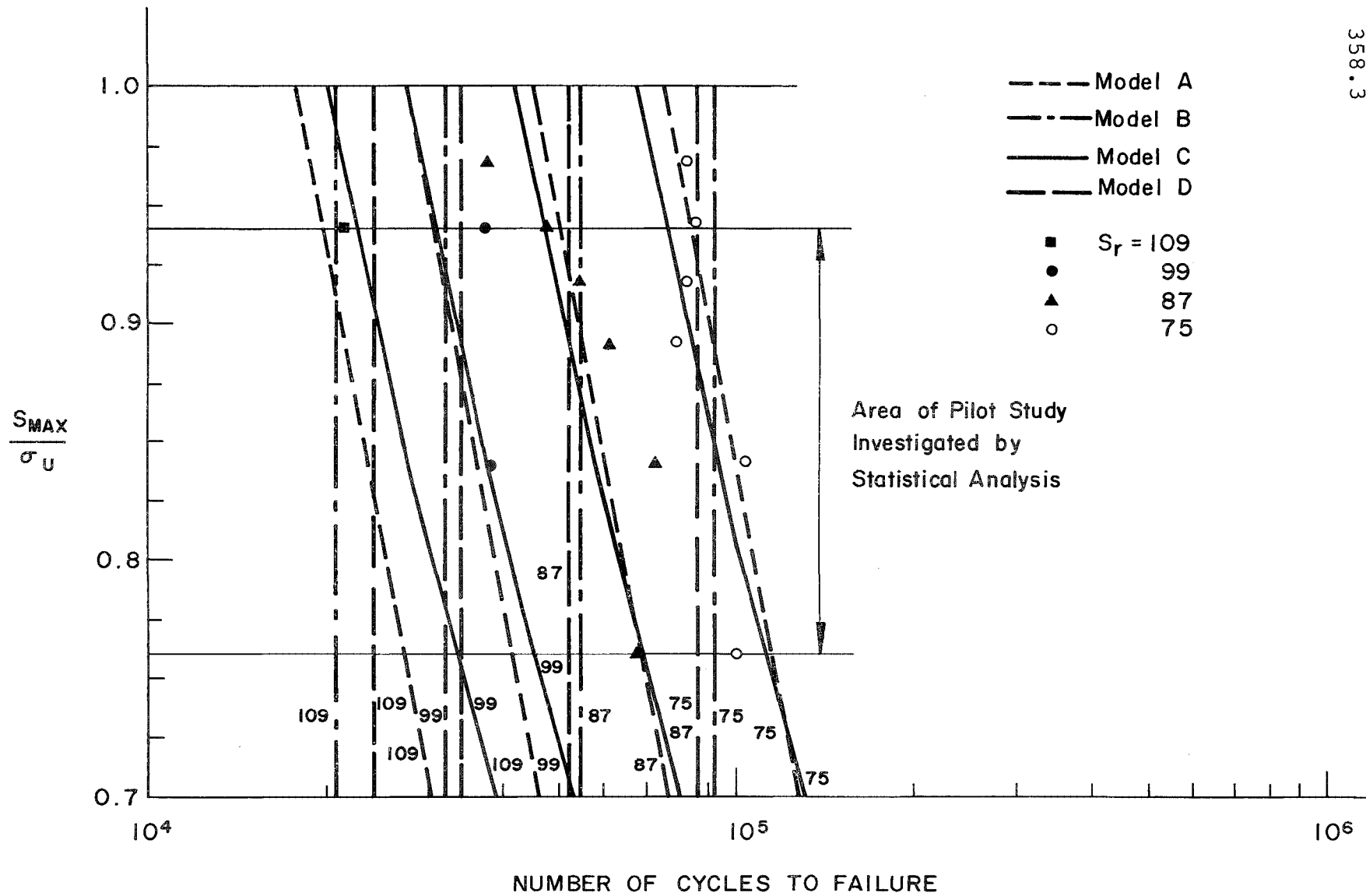


Fig. 14 Maximum Stress Ratio Versus Number of Cycles - Statistically

9. REFERENCES

1. Smith, R. J., Lozano, S., and Marek, P.  
PILOT STUDY ON THE FATIGUE OF TENSILE SPECIMENS - PHASE 1, Fritz Engineering Laboratory Report 358.1, June, 1969.
2. Dubuc, J.  
EFFECT OF MEAN STRESS AND OF MEAN STRAIN IN LOW CYCLE FATIGUE OF A-201 AND T-1 STEELS, Report to Pressure Vessel Research Committee, Ecole Polytechnique, Montreal, Canada, July, 1967.
3. Hirt, M. A., and Fisher, J. W.  
FATIGUE STRENGTH OF ROLLED AND WELDED STEEL I BEAMS, Fritz Engineering Laboratory Report 334.3 (in preparation), Lehigh University.
4. Lozano, S., and Marek, P.  
RESIDUAL STRESSES IN WELDED BEAMS, Fritz Engineering Laboratory Report 358.5, (in preparation) Lehigh University.
5. Nagaraj Rao, N. R., Lohrmann, M., and Tall, L.  
EFFECT OF STRAIN RATE ON THE YIELD STRESS OF STRUCTURAL STEELS, Journal of Materials, Vol. 1, No. 1, March, 1966.
6. Fisher, J. W., Frank, K. H., Hirt, M. A., and McNamee, B. M.  
EFFECT OF WELDMENTS ON THE FATIGUE STRENGTH OF STEEL BEAMS, Fritz Engineering Laboratory Report 334.2, September, 1969 (Final Report for Publication by Highway Research Board as NCHRP Report).
7. Natrella, M. G.  
EXPERIMENTAL STATISTICS, National Bureau of Standards Handbook 91, U.S. Printing Office, Washington, D. C., 1963.

Security Classification

DOCUMENT CONTROL DATA - R & D

(Security classification of title, body of abstract and indexing annotation must be entered when the overall report is classified)

1. ORIGINATING ACTIVITY (Corporate author)		2a. REPORT SECURITY CLASSIFICATION	
		2b. GROUP	
3. REPORT TITLE			
Low Cycle Fatigue PILOT STUDY ON THE FATIGUE OF TENSION SPECIMENS (PHASES 1 AND 2)			
4. DESCRIPTIVE NOTES (Type of report and inclusive dates)			
5. AUTHOR(S) (First name, middle initial, last name)			
R. J. Smith, P. Marek, M. Perlman, A. W. Pense, K. H. Frank, and J. W. Fisher.			
6. REPORT DATE		7a. TOTAL NO. OF PAGES	7b. NO. OF REFS
October, 1969		49	7
8a. CONTRACT OR GRANT NO.		9a. ORIGINATOR'S REPORT NUMBER(S)	
N 00014-68-A-514; NR 064-509			
b. PROJECT NO.		358.3	
c. 358		9b. OTHER REPORT NO(S) (Any other numbers that may be assigned this report)	
d.			
10. DISTRIBUTION STATEMENT			
11. SUPPLEMENTARY NOTES		12. SPONSORING MILITARY ACTIVITY	
13. ABSTRACT			
<p>This report presents a summary and evaluation of the results of a pilot study, which is part of a major research program designed to provide information on the behavior and design of joined structures subjected to low-cycle fatigue.</p> <p>Seventy-one tension specimens were tested to obtain information on the significance of several design factors which may influence the fatigue life of A514 steel from about 10,000 up to 100,000 cycles. In addition, experience was gained concerning the method of testing and the instrumentation required for later tests.</p> <p>The fracture surfaces were characterized and correlations of fatigue life with maximum stress and stress range were tested. When the maximum stress was below the proportional limit it was determined statistically that the stress range accounts for nearly all the variations in cycle life. In regions of high maximum applied stresses, the test data was not sufficient for statistical predictions concerning the effect of the applied stress parameters upon fatigue life.</p> <p>Final fracture of the specimens was initiated by flat fatigue cracks and proceeded by non-homogeneous plastic flow across the specimen. At high loads and high stress ranges, multiple crack initiation was observed and the flat fatigue crack was a smaller portion of the critical fracture surface.</p> <p>For high maximum stresses where "plastic damage" occurs during fatigue, the study has indicated that measurements of plastic strain accumulation during testing will be necessary.</p>			